Informatics in Medicine Unlocked 42 (2023) 101366

Contents lists available at ScienceDirect

Informatics in Medicine Unlocked

journal homepage: www.elsevier.com/locate/imu

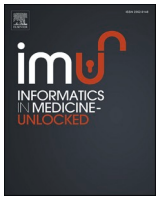

Enhancing stability in cardiovascular disease risk prediction: A deep learning approach leveraging retinal images

Weiyi Zhang [a], Zhen Tian [a], Fan Song [a], Pusheng Xu [b], Danli Shi [a,c,*], Mingguang He [a,b,c]

[a] School of Optometry, The Hong Kong Polytechnic University, Kowloon, Hong Kong SAR, China
[b] State Key Laboratory of Ophthalmology, Zhongshan Ophthalmic Center, Sun Yat-sen University, Guangdong Provincial Key Laboratory of Ophthalmology and Visual Science, Guangdong Provincial Clinical Research Center for Ocular Diseases, Guangzhou, 510060, China
[c] Research Centre for SHARP Vision, The Hong Kong Polytechnic University, Kowloon, Hong Kong SAR, China

ARTICLE INFO

Keywords:
Cardiovascular disease
Retinal imaging
Artificial intelligence
Risk estimation

ABSTRACT

Background: The retina provides valuable insights into vascular health within the body. Prior studies have demonstrated the potential of deep learning in predicting Cardiovascular Disease (CVD) risk using color fundus photographs.

Purpose: To use fundus images to more consistently predict the World Health Organization (WHO) CVD score and to address the problem of year-to-year fluctuations associated with the traditional CVD risk score calculation.

Methods: Utilizing 55,540 fundus images from 3,765 participants with 6-year follow-up data, we designed a DL model named Reti-WHO based on the Swin Transformer to predict CVD risk regression scores. Multiple regression and classification metrics such as coefficient of determination (R2-score), Mean Absolute Error (MAE), sensitivity and specificity were employed to assess the accuracy of the Reti-WHO. Significance differences between WHO CVD scores and Reti-WHO scores were also assessed. Vessel measurements were employed to interpret the model and evaluate the association between Reti-WHO and vascular conditions.

Results: The deep learning model achieved good classification and regression metrics on the validation set, with an R2-score of 0.503, MAE of 1.58, sensitivity of 0.81, and specificity of 0.66. There was no statistically significant difference between WHO CVD scores and Reti-WHO scores (P value = 0.842). The model exhibited a stronger correlation with vascular measurements, including mean and variance of arc and chord in arteries and veins. Comparing box plots and Vyshyvanka plots depicting changes in patients' CVD over the years, the Reti-WHO calculated by our model demonstrated greater stability compared to non-deep learning-based WHO CVD risk calculations.

Conclusions: Our Reti-WHO scores demonstrated enhanced stability compared to WHO CVD scores calculated solely from the patient's physical indicators, suggesting that the features learned from retinal fundus photographs serve as robust indicators of CVD risk. However, the model may still exhibit false negatives in high-risk predictions, requiring ongoing research for refinement. Future directions involve validating the model across diverse populations and exploring multi-image and multi-modal approaches to enhance prediction accuracy.

1. Introduction

Cardiovascular Disease (CVD) is the leading cause of morbidity and mortality globally [1], with reported cases increasing from 271 million in 1990 to 523 million in 2019 [2]. The pathogenesis of CVD involves multiple factors, such as exosomes [3], fibrinogen [4], and others. In addition, several well-known risk factors, including hypertension, obesity, and smoking, contribute to the increased incidence of CVD [4]. Fortunately, regular screening of the at-risk populations and control of risk factors can help reduce the incidence of CVD events and prevent cardiovascular complications [5]. Various CVD risk calculators, such as the Framingham Cardiovascular Risk Score [6], Systemic Coronary Risk Evaluation (SCORE) [7] and the Pooled Cohort Equation (PCE) [8], have been developed. However, these models often lack validation due to their reliance on data from small population samples, primarily from developed countries [9–11]. As a result, there is a need to improve risk prediction models for more diverse populations. To address this limitation, the World Health Organization (WHO) has developed, evaluated

* Corresponding author. School of Optometry, The Hong Kong Polytechnic University, Kowloon, Hong Kong SAR, China
E-mail address: danli.shi@polyu.edu.hk (D. Shi).

https://doi.org/10.1016/j.imu.2023.101366
Received 28 July 2023; Received in revised form 13 September 2023; Accepted 26 September 2023
Available online 27 September 2023

and illustrated revised risk models for predicting CVD risk in low and middle-income countries [12], incorporating traditional cardiovascular risk factors such as systolic blood pressure, diabetes history, total cholesterol, smoking status, and age. However, the reliance on such factors may lead to fluctuations in risk scores over time.

The retina, with its high vascularity and noninvasive accessibility through imaging, serves as a surrogate measure for evaluating systemic vascular health [13]. Extensive studies have highlighted the valuable information on cardiovascular health contained in fundus images [14]. For example, a previous study demonstrated a strong correlation between retinal vascular fractal dimension and the risk of heart failure [15].

Leveraging Color Fundus (CF) photographs for predicting CVD risk offers several advantages, including non-invasiveness and convenience for screening large populations [16]. Deep learning algorithms have shown their predictive value in assessing cardiovascular risk factors and major adverse events using retinal fundus images [17]. By considering vascular information, such as changes in blood vessel size and shape in the retina [18], these algorithms address aspects often overlooked by traditional risk assessment methods. Previous studies have successfully demonstrated the feasibility of CVD risk prediction using fundus photographs[19 20].

In this study, we address an important issue observed in a cohort of Chinese civil servants, where the WHO CVD risk score exhibited significant fluctuations for the same patient in different years of follow-up data, deviating from clinical experience. To tackle this discrepancy, we propose a CF-based deep learning approach to predict a WHO CVD risk score, assuming retinal photographs can serve as a more stable indicator of end-organ damage.

The primary objective of this study is to develop a deep learning algorithm (termed Reti-WHO) for predicting CVD risk scores using retinal photographs. Unlike existing methods, Reti-WHO aims to address the challenge of stability in CVD risk prediction within the same individual over time. Additionally, we explore the model's ability to establish a robust connection between retinal features and cardiovascular health by examining its correlation with vascular variables. Through this research, we aim to demonstrate that leveraging retinal images for CVD risk assessment not only provides stable and consistent results within individuals but also establishes a significant association with vascular variables, thus showcasing the unique contributions of the Reti-WHO model in the field of CVD risk prediction.

2. Methods

2.1. Study population

In this study, we used the clinical data and retinal photographs with six-year annual follow-up in China. To ensure data quality, we performed a two-step quality control process. Firstly, patients with missing or aberrant outlier values in factors such as age, smoking status, blood pressure, history of diabetes, and total cholesterol level were excluded from the analysis to ensure that we could accurately calculate WHO CVD risk. Secondly, we conducted a quality control process to remove low-quality retinal images with insufficient segmented vessels, identified by a low vessel-to-background ratio. We divided each image into four quadrants and filtered out images with more than two quadrants exhibiting a vessel-to-background ratio below 4%. This step helped to maintain a dataset with high-quality retinal images that possessed the necessary features for accurate CVD risk prediction. The number of images and patients excluded through the quality control process is presented in Fig. 2. The final dataset comprised 4,205 participants with follow-up periods ranging from 1 to 6 years. Each participant's annual follow-up data included two fundus images for both the right and left eyes. To mitigate potential biases in the dataset, we employed stratified sampling to divide the dataset at the patient level into a training set (60%), a validation set (20%), and a test set (20%). This stratified approach ensured that each subset maintained a balanced distribution of risk levels, addressing potential biases and enhancing the robustness of our model.

2.2. Calculation of the baseline WHO CVD risk scores

We calculated reference WHO CVD scores using a recently calibrated model [12] based on data from multiple countries. The model aims to predict the 10-year risk of fatal and non-fatal cardiovascular diseases, such as myocardial infarction and stroke. It incorporates information strongly associated with cardiovascular diseases, including age, smoking status, systolic blood pressure, history of diabetes, and total cholesterol level.

2.3. Retinal-based deep learning CVD prediction model

In this study, we developed a deep learning-based model called Reti-WHO to predict CVD risk. In the preprocessing phase, for each fundus image, we subtracted the local mean from a 4 × 4-pixel neighbourhood and placed it on a dark background in a square image with strict boundaries [19]. Fig. 1 shows the samples of the original and pre-processed images. We also applied data enhancement techniques such as random horizontal flipping, random zoom-in and zoom-out, and random luminance and contrast perturbations to enhance the robustness of the model.

We used Swin Transformer [20] as the deep learning model, with input fundus images resized to 224x224. The Swin Transformer's distinctive architecture, characterized by its utilization of hierarchical and shifted windows, demonstrated remarkable efficacy in capturing intricate image patterns. This architectural advantage was particularly beneficial for our task of analyzing retinal fundus photographs, which encompass intricate vascular structures and nuanced features relevant to cardiovascular health. Additionally, the Swin Transformer's capacity to manage extensive image datasets while efficiently utilizing memory resources rendered it well-suited for our dataset, comprising a substantial volume of high-resolution fundus images.

To speed up the training, model weights were initialized using ImageNet [18] weights. The model was trained by 20 epochs with a learning rate of 1e-4 and a batch size of 8. The weights of all layers except the last layer were frozen, and an Adam optimizer was used to optimize training. The model with the best model performance (R2-score) on the validation set was selected for testing. The open-source software library Pytorch was used for training and evaluation.

2.4. Performance evaluation metrics

To assess the effectiveness of the Reti-WHO model, we employed various regression evaluation metrics, including the coefficient of determination (R2-score), Mean Absolute Error (MAE), Root-Mean-Square Error (RMSE), and correlation coefficient. The R2-score assesses the proportion of variance in the CVD risk explained by the model. It provides insight into how well the model captures the underlying patterns and trends in CVD risk. MAE and RMSE are valuable metrics for evaluating the magnitude of prediction errors. MAE measures the average absolute difference between the predicted and actual risk scores, providing a straightforward assessment of prediction accuracy. RMSE, on the other hand, penalizes larger errors more heavily, giving a sense of the model's performance in handling outliers or extreme predictions. The correlation coefficient quantifies the strength and direction of the linear relationship between the predicted and actual CVD risk scores. It indicates how well the model's predictions align with the true risk values, providing valuable insights into the model's predictive power and consistency. We also assess the statistical differences between WHO CVD scores and Reti-WHO scores to provide evidence for the distinction between the two scoring systems.

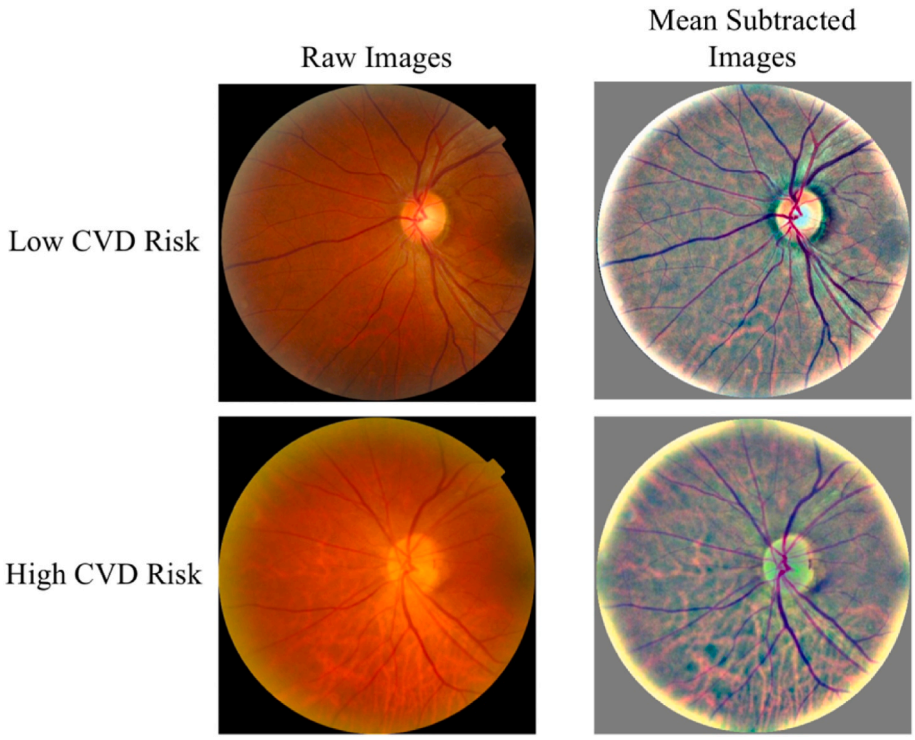

Fig. 1. Example of color fundus images before and after pre-processing. Our preprocessing technique is to subtract the average color of each retinal image. (For interpretation of the references to color in this figure legend, the reader is referred to the Web version of this article.)

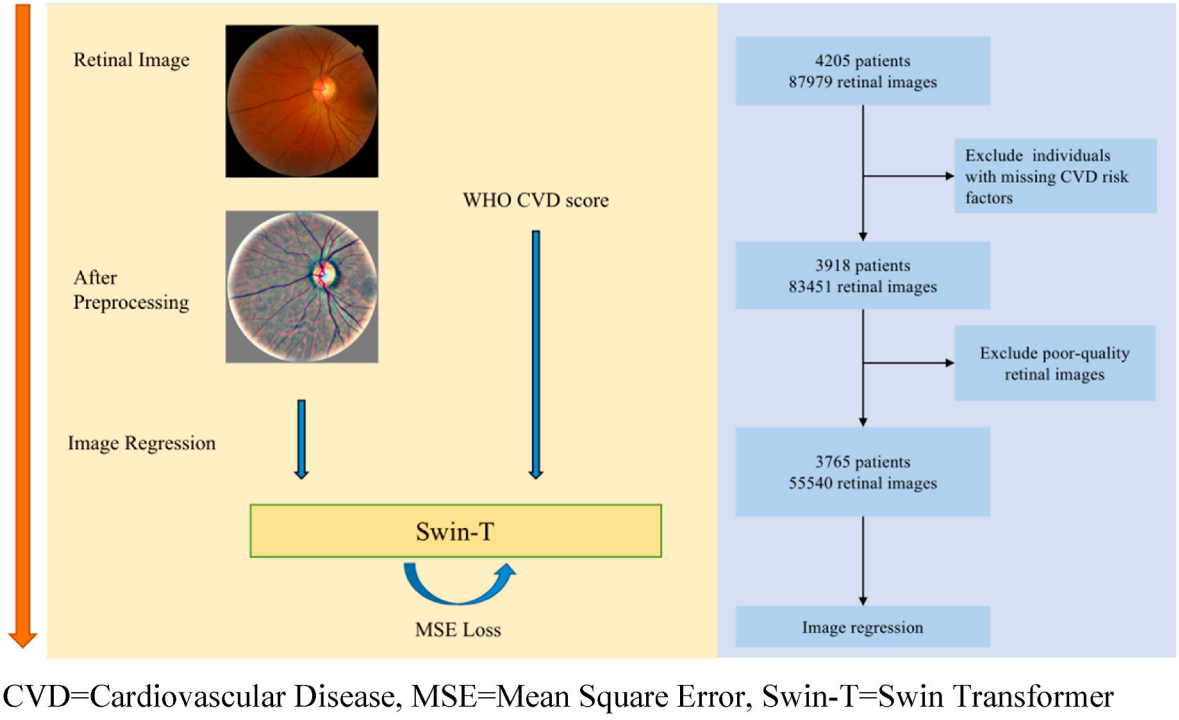

Fig. 2. Flowchart of the study.
CVD=Cardiovascular Disease, MSE = Mean Square Error, Swin-T = Swin Transformer.

Additionally, we conducted binary classification based on the regression scores, using a threshold of 15 between low & borderline-risk and high-risk categories [12]. Several classification metrics, including accuracy, precision, sensitivity, specificity, and F1 score were used to evaluate the quality of classification. Accuracy provides an overall view of classification performance, while precision focuses on minimizing false positives, sensitivity on minimizing false negatives, and specificity on accurately classifying low-risk individuals. The F1 score strikes a balance between precision and sensitivity, making it particularly valuable when minimizing both false positives and false negatives is crucial.

These metrics provide a comprehensive assessment of the Reti-WHO model's performance in CVD risk prediction, encompassing precision in risk estimation and accuracy in risk category classification, offering a holistic view of its alignment with research objectives.

2.5. Correlation analysis

To visualize the stability and progression over time, we plotted box plots and Vyshyvanka plots of both WHO CVD risk scores and Reti-WHO scores. The plots were organized according to the year of patients in the test set, with each patient forming a distinct group.

To assess the relationship between vascular indices and Reti-WHO and WHO CVD scores across different risk levels, we considered a total of 627 vascular measurement indices, including arc, tortuosity [21], branching coefficient [22]' and caliber, obtained from retinal blood vessel segmentation. The correlation coefficients between these parameters were calculated to evaluate their associations. Correlation coefficients were calculated to evaluate these associations, and statistical measures were used to analyze the characteristics of different risk levels determined by Reti-WHO and WHO CVD scores.

2.6. Attention visualization

To improve the interpretability of the deep learning model and gain insights into its decision-making process, we employed the integrated gradient attention visualization method [23]. This method involves visualizing and analyzing the model by calculating the gradients of multiple fractions obtained by adding up the differences between an all-black image and the input image. The gradients are then averaged to determine the regions of interest in the model's predictions, helping to interpret its judgments and focus areas.

3. Results

3.1. Characteristics of participants and distribution of retinal images

The study included a total of 3,765 subjects, with 55,540 fundus images analyzed. Table 1 presents the participants' characteristics. The mean (standard deviation) age of the subjects at the baseline year (2010) was 58.88 (±8.38) years, with a higher proportion of male participants (59.10%). The average BMI showed a statistically significant increase in the years 2011–2015 compared to the baseline year. Table 2 presents the distribution of retinal images within the dataset, categorized according to different risk levels based on the WHO CVD Risk Chart Working Group [12]. The dataset was split into training, validation, and test sets, with consistent proportions of risk levels maintained within each subset. Approximately 70% of the retinal images were classified as CVD high risk, 23% as CVD low risk, and the remaining as borderline risk, ensuring a balanced dataset for model training and evaluation.

3.2. Reti-WHO performance and comparison with WHO CVD scores

As shown in Table 3, the deep learning model Reti-WHO demonstrated impressive performance on the test set. When compared to the WHO CVD risk score calculated using physical data, Reti-WHO showcases an R2-score of 0.503, an MAE of 1.58, and a correlation coefficient of 0.710. There was no significant difference between WHO CVD scores and Reti-WHO scores (t-test P value = 0.842). These results highlight the informative insights of our deep learning model in predicting CVD risk.

The binary classification results further underscore the effectiveness of Reti-WHO in assessing risk levels. With an overall accuracy of 0.82, Reti-WHO demonstrates its ability to accurately classify individuals into appropriate risk categories. Particularly noteworthy is its robust performance in identifying high-risk individuals, achieving an accuracy of 0.96 and a sensitivity of 0.96. This high accuracy and sensitivity ensure the reliability of Reti-WHO in detecting individuals with an elevated risk of developing CVD, significantly reducing the chances of false negatives.

Fig. 3 illustrates a comparison of box plots and Vyshyvanka plots depicting the CVD risk of participants based on age, comparing Reti-WHO to WHO CVD scores. Fig. 3 (a) reveals that Reti-WHO has a narrower range, more tightly distributed data, and fewer outliers compared to WHO CVD scores. The Vyshyvanka plot shown in Fig. 3 (b) demonstrates that Reti-WHO exhibits less fluctuation in risk scores for the same participant across different years, indicating its stability and robustness.

3.3. Correlation analysis of vascular measurements with Reti-WHO and WHO CVD scores

Fig. 4 presents the correlation coefficients between (a) arterial-related measurement indices, (b) venous-related measurement indices, and both Reti-WHO and WHO CVD scores. Firstly, there is a strong association between these two CVD risk scores and vascular measurements, such as the mean and variance of arc and chord in arteries and veins. Secondly, the correlation between Reti-WHO and vascular measurements, predicted from retinal images, is significantly stronger than the correlation observed between WHO CVD scores and vascular measurements.

Table 4 presents the statistical analysis of mean and variance for

Table 1
Characteristics of all participants (n = 3765).

Characteristics(n = 3765)	Mean (SD)/n (%)					
	Baseline year (n = 3490)	First year follow-up (n = 2739)	Second year follow-up (n = 2576)	Third year follow-up (n = 2479)	Fourth year follow-up (n = 2397)	Fifth year follow-up (n = 2344)
Age	60.58(8.78)	62.86(7.54)	63.85(7.56)	64.79(7.42)	65.67(7.41)	66.28(7.41)
Gender, male	8581 (58.62%)	6591(60.82%)	6421(60.86%)	6188(61.2%)	6074(60.69%)	5572(58.73%)
BMI, kg/m2	24.04(2.97)	24.45(3.12)	24.3(3.13)	24.22(3.09)	24.21(3.2)	24.23(3.13)
Systolic blood pressure, mm Hg	129.16 (18.01)	128.79(16.9)	127.74(16.59)	127.83(16.4)	128.59(16.05)	128.95(15.97)
Diastolic blood pressure, mmHg	75.06 (11.31)	71.51(11.02)	71.24(11.2)	71.13(10.45)	72.1(10.24)	72.22(10.2)
Total cholesterol, mmol/L	5.45(0.92)	5.94(1.14)	5.35(1.05)	5.47(1.04)	5.31(1.05)	5.47(1.05)
Smoking, yes	2854 (19.5%)	2042(18.84%)	2045(19.38%)	1990(19.68%)	1898(18.96%)	1735(18.29%)
Serum glucose, mmol/L	5.59(1.16)	5.97(1.38)	5.8(1.44)	6.03(1.44)	6.17(1.66)	6.17(1.53)
Diabetes, yes	1937 (13.23%)	2238(20.65%)	2489(23.59%)	2610(25.81%)	2887(28.85%)	2919(30.77%)

BMI: Body Mass Index.

Table 2
The train, validation and test dataset characteristics.

	Num of Participants	Num of Images (%)			
		Total	Low Risk(WHOCVD<10)	Borderline Risk(10 ≤ WHOCVD<15)	High Risk(WHOCVD ≥ 15)
Train Set	2259	33366	7671 (22.99%)	2726 (8.17%)	22969 (68.84%)
Validation Set	753	11420	2674 (23.42%)	754 (6.60%)	7992 (69.98%)
Test Set	753	10754	2499 (23.24%)	827 (7.69%)	7428 (69.07%)
Total	3765	55540	12844 (23.13%)	4307 (7.75%)	38389 (69.12%)

Table 3
Performances of Reti-WHO compared with the baseline WHO CVD risk scores.

Regression					
	R2-Score	MAE	RMSE	Correlation Coefficient	P value[a]
	0.503	1.58	1.99	0.710	0.842
Binary Classification					
	Accuracy	**Precision**	**Sensitivity**	**Specificity**	**F1-Score**	**N**
Low Risk (WHO CVD<15)	0.52	0.85	0.52	0.96	0.65	2946
High Risk(WHO CVD>=15)	0.96	0.82	0.96	0.52	0.88	6552
Weighted Avg	0.82	0.82	0.81	0.66	0.81	9498

[a] Student t-test.

vascular measurement values across different risk levels. Subsection (a) focuses on the relationship between WHO CVD risk levels and vascular measurements, while subsection (b) examines the association between Reti-WHO risk levels and vascular measurements. Notably, an interesting observation arises from the Reti-WHO results, where the differences in vascular measurement values between different risk levels are larger. This implies that Reti-WHO has a stronger ability to differentiate the vascular condition among different risk levels, providing a more distinct separation between them.

3.4. Visual analysis

Fig. 5 presents visual analyses of two retinal image cases. The calculation of retinal vessel tortuosity involves measuring the curve length of a blood vessel segment and dividing it by the length between the start and end points of that segment. This method allows for the quantification of the degree of curvature or winding of the blood vessel. In the first case, both the WHO CVD score and Reti-WHO classified the individual as high risk, while in the second case, the WHO CVD score indicated low risk, whereas Reti-WHO classified it as high risk. An experienced ophthalmologist (F.S.) carefully reviewed the images, noting abnormal tortuosity and narrowed artery caliber, as observed in the tortuosity map and caliber map in the second case. These findings further support the more reasonable high CVD risk classification by Reti-WHO.

Fig. 6 displays the attention visualization results of our deep learning model for predicting CVD risk scores based on retinal images. It can be observed that our model tends to focus on the optic disc region and regions with abundant blood vessels. This reaffirms the strong correlation between Reti-WHO and vascular information.

4. Discussion

In conclusion, our study introduces Reti-WHO, an innovative deep learning algorithm designed to accurately predict cardiovascular disease (CVD) risk using retinal fundus photographs. What sets our approach apart from existing methods are two key differentiators. First, we employ the Swin Transformer, a vision transformer architecture, as the backbone of our model. This choice contrasts with the prevalent use of Convolutional Neural Network (CNN) models in the field of predicting CVD risk from retinal images [17,24,25], offering several advantages. The transformer architecture excels in capturing complex patterns within images, making it particularly suited for the intricate vascular structures and subtle features relevant to cardiovascular health present in retinal images. Its hierarchical and shifted windows approach allows for effective feature extraction, enabling Reti-WHO to discern subtle variations that may be overlooked by traditional CNN-based models. This superior ability to capture fine-grained details in retinal images translates into more accurate and robust CVD risk predictions. Second, our study provides evidence that utilizing retinal images for CVD risk prediction yields more stable and consistent results within the same subjects. Importantly, our findings establish a strong correlation between our model's predictions and vascular variables, a relationship not explored by other methods. This underscores the untapped potential of retinal images in predicting CVD risk and highlights the unique contribution of our approach. By leveraging these two distinguishing features, Reti-WHO surpasses traditional WHO CVD score calculations in terms of performance, reliability, and stability. It equips clinicians and patients with a powerful tool for assessing and managing cardiovascular risk, offering valuable insights into proactive interventions and personalized care.

Further analysis reveals three key aspects. Firstly, our results demonstrate that our proposed method of using deep learning to predict CVD risk from retinal images is more stable and has a longer-term reference value than CVD risk values calculated using tabular body data. Numerous studies have shown that short-term habit changes can have a significant impact on certain indicators in the body. For example, Ankad et al. [26] found that short-term (15 days) regular pranayama and meditation resulted in significant reductions in resting pulse rate, systolic blood pressure, diastolic blood pressure, and mean arterial blood pressure, which indirectly affected the WHO CVD risk calculations, but this short-term benefit did not mean that the participants' cardiovascular disease risk was substantially reduced. In addition, the presence or absence of smoking or alcohol consumption is a highly uncertain factor in the calculation of the WHO CVD risk value, as the participant's risk of CVD would not theoretically have been significantly reduced if he or she had just quit smoking or drinking at the time of information collection, but the WHO CVD risk value calculated traditionally would be influenced by the indicator. In contrast, the retinal fundus image does not change significantly in the short term, except for pathological changes or changes due to trauma, and is also highly sensitive to individual exogenous factors such as high air pollution that trigger CVD [27]. These characteristics suggest that the use of fundus images to predict CVD risk will be a more stable and reliable technique,

(a) Box plot.

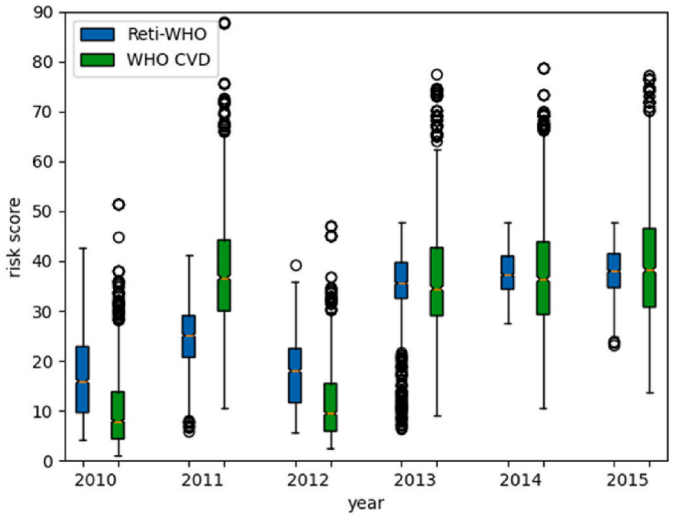

(b) Vyshyvanka plot; Upper: WHO CVD Risk Scores; Lower: Reti-WHO Risk Scores.

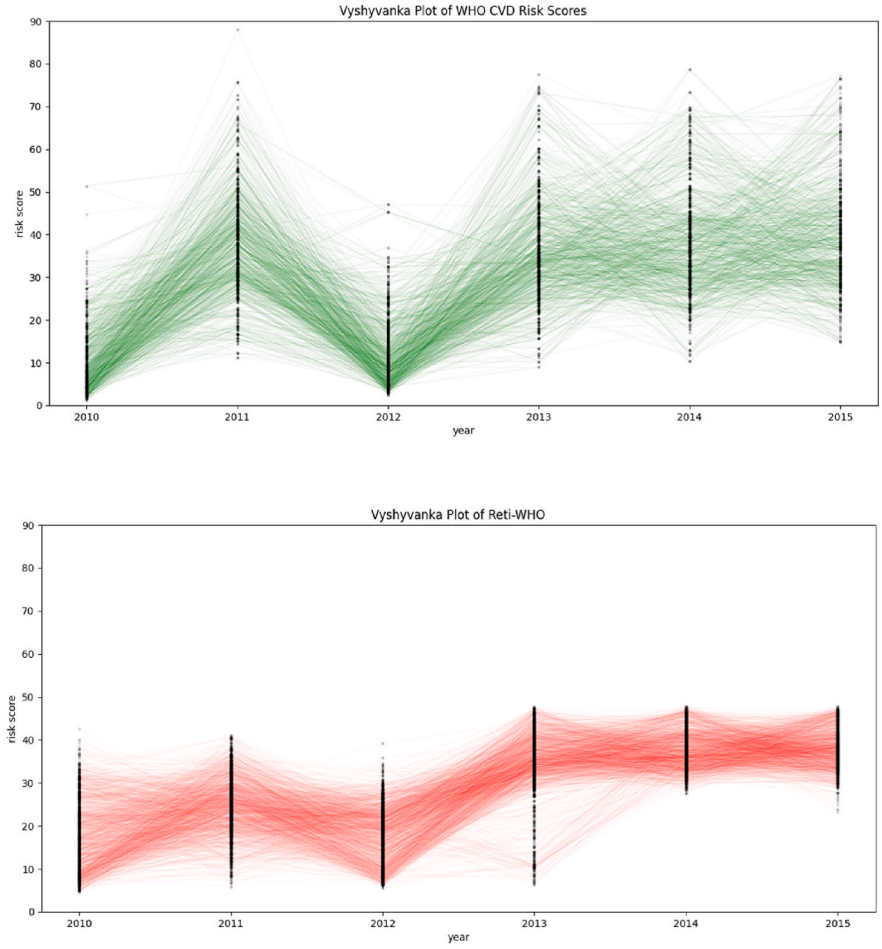

Fig. 3. Box plots and Vyshyvanka plots of the annual cardiovascular disease risk of participants by Reti-WHO versus WHO CVD scores.

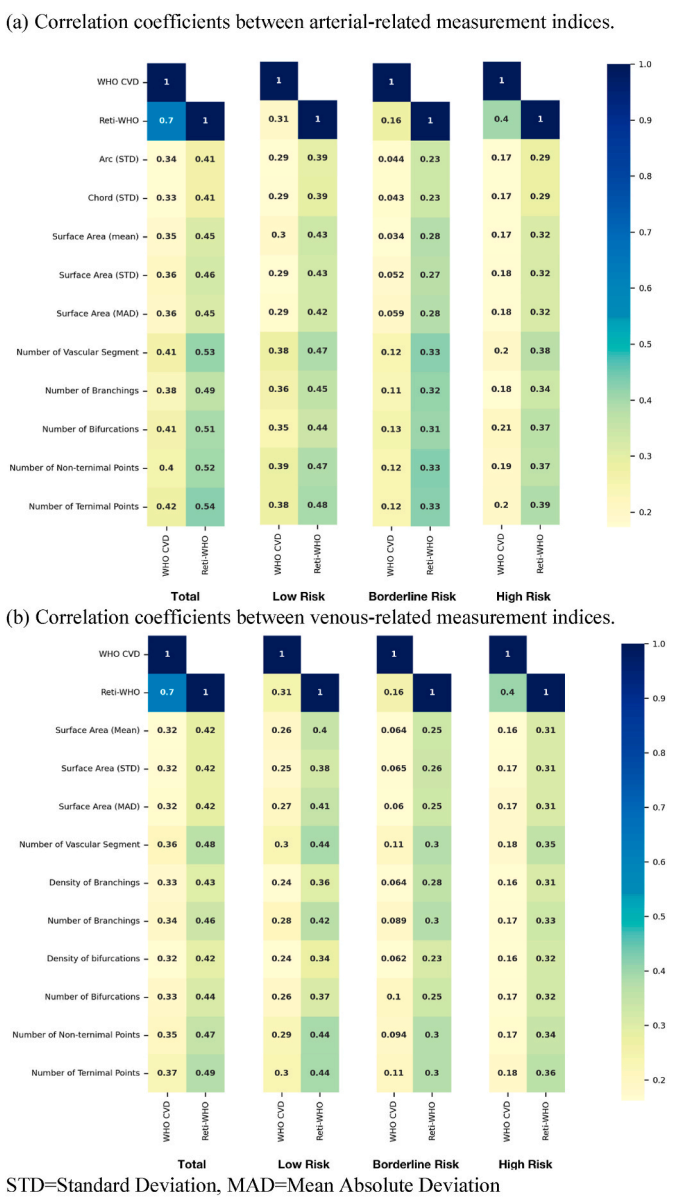

Fig. 4. Correlation coefficients between (a) arterial-related measurement indices, (b) venous-related measurement indices, and both Reti-WHO and WHO CVD scores. The column labeled "Total" includes all patients in the study, "Low risk" corresponds to patients with WHO CVD risk scores ≤15, "Borderline risk" to scores >10 but <15, and "High risk" to scores ≥15.
STD=Standard Deviation, MAD = Mean Absolute Deviation.

which is consistent with our findings.

Secondly, our study demonstrates that our deep learning approach utilizing retinal images outperforms traditional CVD risk scores in terms of correlation with vascular measurements. Multiple studies in the literature have emphasized the association between retinal vasculature and cardiovascular diseases. Wong et al. conducted a comprehensive investigation into retinal microvascular abnormalities and their connection with hypertension, cardiovascular disease, and mortality. Their research yielded compelling evidence of a significant link between retinal vascular abnormalities and adverse cardiovascular outcomes, thereby providing critical support for the relevance of retinal vasculature in the assessment of CVD risk [28]. Roy et al. concentrated on elucidating the relationship between retinal vessel caliber and cardiovascular disease and mortality among African Americans with type 1 diabetes mellitus. Their study further underscored the importance of

Table 4
Mean and variance analysis of vascular measurement values across different risk levels.

(a)Statistical analysis of vascular measurement values across WHO CVD risk levels.

Vessel Measurement	Total	Low Risk	Borderline Risk	High Risk
Arc (std)	125.25 (40.96)	101.86 (25.63)	119.99 (34.14)	132.80 (42.56)
Chord (std)	115.28 (38.32)	93.44 (24.01)	110.35 (32.00)	122.33 (39.82)
Surface Area (Mean)	578.39 (172.06)	474.53 (110.01)	553.31 (143.72)	612.01 (176.95)
Surface Area (Standard Deviation)	589.50 (181.05)	476.04 (122.89)	560.46 (151.03)	626.62 (183.74)
Surface Area (Mean Absolute Difference)	437.03 (144.63)	348.09 (96.13)	415.86 (122.39)	466.02 (147.52)
Number of Vascular Segment	114.38 (47.91)	150.68 (43.80)	118.39 (41.28)	103.02 (44.04)
Number of Branchings	66.77 (33.77)	90.84 (32.09)	69.01 (29.53)	59.28 (31.13)
Number of Bifurcations	43.38 (17.80)	56.38 (16.16)	45.04 (15.73)	39.32 (16.52)
Number of Non-terminal Points	57.67 (25.58)	76.61 (23.62)	59.69 (22.21)	51.75 (23.58)
Number of Terminal Points	63.23 (25.16)	82.59 (23.10)	65.43 (21.53)	57.16 (23.00)
Surface Area (Mean)	580.29 (166.97)	487.99 (93.29)	558.59 (145.83)	609.11 (175.33)
Surface Area (Standard Deviation)	620.01 (187.74)	515.88 (112.00)	598.26 (157.81)	652.88 (196.58)
Surface Area (Mean Absolute Difference)	442.26 (145.14)	361.54 (82.25)	425.13 (124.18)	467.66 (152.45)
Number of Vascular Segment	146.55 (52.39)	180.99 (44.25)	149.97 (47.40)	135.82 (50.57)
Density of Branchings	0.01 (0.00)	0.01 (0.00)	0.01 (0.00)	0.01 (0.00)
Number of Branchings	89.67 (38.08)	113.82 (33.44)	91.69 (34.98)	82.17 (36.60)
Density of bifurcations	0.01 (0.00)	0.01 (0.00)	0.01 (0.00)	0.01 (0.00)
Number of Bifurcations	52.26 (18.20)	63.26 (15.72)	53.51 (16.57)	48.83 (17.71)
Number of Non-terminal Points	72.71 (27.76)	90.80 (23.70)	74.17 (25.02)	67.11 (26.79)
Number of Terminal Points	80.35 (27.48)	98.85 (23.29)	82.43 (24.91)	74.55 (26.37)

(b) Statistical Analysis of vascular measurement values across Reti-WHO risk levels.

Vessel Measurement	Total	Low Risk	Borderline Risk	High Risk
Arc (std)	125.25 (40.96)	91.20 (17.61)	103.31 (24.68)	131.27 (41.53)
Chord (std)	115.28 (38.32)	83.51 (16.31)	94.74 (22.99)	120.89 (38.88)
Surface Area (Mean)	578.39 (172.06)	425.00 (67.88)	478.92 (104.39)	605.48 (173.00)
Surface Area (Standard Deviation)	589.50 (181.05)	421.25 (80.41)	482.05 (114.45)	619.29 (180.30)
Surface Area (Mean Absolute Difference)	437.03 (144.63)	304.39 (61.58)	353.63 (89.83)	460.43 (144.65)
Number of Vascular Segment	114.38 (47.91)	173.22 (35.65)	145.60 (40.86)	104.61 (43.50)
Number of Branchings	66.77 (33.77)	107.00 (27.37)	87.19 (30.14)	60.18 (30.68)
Number of Bifurcations	43.38 (17.80)	63.75 (13.95)	54.75 (15.03)	39.97 (16.40)
Number of Non-ternimal Points	57.67 (25.58)	88.89 (19.44)	74.16 (22.12)	52.49 (23.21)
Number of Ternimal Points	63.23 (25.16)	94.55 (19.01)	79.73 (21.24)	58.03 (22.75)
Surface Area (Mean)	580.29 (166.97)	445.79 (51.08)	489.09 (87.22)	603.05 (171.12)
Surface Area (Standard Deviation)	620.01 (187.74)	468.13 (72.09)	523.42 (108.15)	645.91 (191.70)

(*continued on next page*)

Table 4 (*continued*)

(b) Statistical Analysis of vascular measurement values across Reti-WHO risk levels.

Vessel Measurement	Total	Low Risk	Borderline Risk	High Risk
Surface Area (Mean Absolute Difference)	442.26 (145.14)	323.34 (45.64)	365.53 (77.75)	462.56 (148.61)
Number of Vascular Segment	146.55 (52.39)	203.90 (34.72)	176.72 (42.05)	137.06 (49.66)
Density of Branchings	0.01 (0.00)	0.01 (0.00)	0.01 (0.00)	0.01 (0.00)
Number of Branchings	89.67 (38.08)	130.47 (27.36)	110.88 (32.12)	82.93 (35.97)
Density of bifurcations	0.01 (0.00)	0.01 (0.00)	0.01 (0.00)	0.01 (0.00)
Number of Bifurcations	52.26 (18.20)	70.09 (13.10)	61.63 (14.87)	49.33 (17.53)
Number of Non-ternimal Points	72.71 (27.76)	102.90 (18.88)	88.54 (22.52)	67.72 (26.30)
Number of Ternimal Points	80.35 (27.48)	110.99 (18.47)	96.32 (21.99)	75.29 (25.94)

retinal vascular measurements as potential biomarkers for predicting cardiovascular outcomes, reaffirming the pertinent role of retinal vasculature in CVD risk assessment [29]. In light of the existing body of knowledge, our research advances the field by utilizing deep learning to develop Reti-WHO based on retinal images. By doing so, we effectively bridge the gap between deep learning models and the well-established association between retinal vasculature and CVD risk. We not only enhance the interpretability of deep learning in cardiovascular research but also extend its practical applicability in this domain. Moreover, our study validates the reliability and significance of Reti-WHO's predictions by leveraging deep learning results. This validation process strengthens the link between retinal vasculature and CVD risk, yielding valuable insights for future research endeavors and clinical applications. The utilization of deep learning to predict CVD risk based on retinal images empowers clinicians with a deeper understanding of an individual's cardiovascular risk profile, thus facilitating proactive intervention and personalized care. Additionally, with further validation studies, Reti-WHO holds promise for its application in large-scale population CVD risk screening to identify individuals at high risk and optimize the allocation of limited medical resources.

Thirdly, our study also demonstrated the efficacy of retinal data in predicting CVD risk. In contrast to traditional high-risk Systemic Coronary Risk Estimation (SCORE) chart estimating the 10-year risk of fatal CVD, which rely on multiple variables such as age, gender, and cholesterol [4], the use of retinal photographs in generating Reti-WHO offers a safe, fast, and effective alternative. This study is, therefore, valuable to practitioners interested in using retinal photographs to predict CVD risk and to those interested in combining traditional and novel methods for CVD risk assessment.

Despite the promising results obtained in our studies, it is important to acknowledge several limitations. Firstly, Reti-WHO still exhibits false negatives in identifying individuals at high risk of CVD, which may be attributed to data limitations, leading to a lack of representation of certain high-risk patterns, and model complexity, where extracted features from retinal images may not fully encompass all relevant information related to high-risk CVD cases. To improve accuracy, future research can focus on data augmentation, transfer learning, and ensemble methods. Addressing these aspects is crucial for enhancing the algorithm's performance in accurately detecting high-risk individuals. Secondly, further validation on cohorts with documented CVD events is necessary to assess the real-world applicability and effectiveness of Reti-WHO in clinical settings. This validation will help assess how well the model's predictions align with actual cardiovascular outcomes and provide valuable insights into its practical utility. Additionally, to enhance the generalizability of the model, it would be valuable to incorporate datasets from diverse ethnicities. Validation across different demographic groups can help validate the robustness and reliability of Reti-WHO in predicting CVD risk more comprehensively. Addressing these limitations will be crucial in realizing the full potential of Reti-WHO as a valuable tool for cardiovascular risk assessment in clinical practice.

5. Conclusion

In conclusion, our work lays the groundwork for a reliable and effective model utilizing retinal images for CVD risk assessment. While promising, ongoing investigation and refinement such as data augmentation and validation in diverse populations are essential to ensure its applicability and impact in clinical practice.

Funding

The study was supported by the Global STEM Professorship Scheme (P0046113). The sponsor or funding organization had no role in the design or conduct of this research.

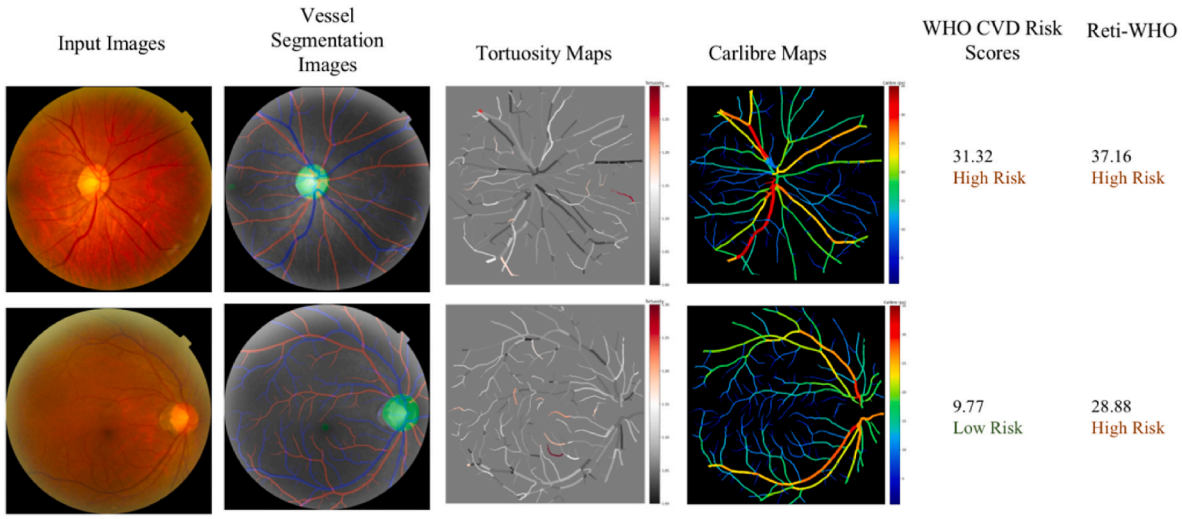

Fig. 5. Examples of visual analyses. The first case shows high-risk classifications for both WHO CVD score and Reti-WHO. The second case demonstrates a low-risk classification based on WHO CVD score but high-risk classification based on Reti-WHO. Images with discrepancies were reviewed by an ophthalmologist, those with higher Reti-WHO than original WHO CVD demonstrated unhealthy vessels with attenuated retinal arteries and increased tortuosity.

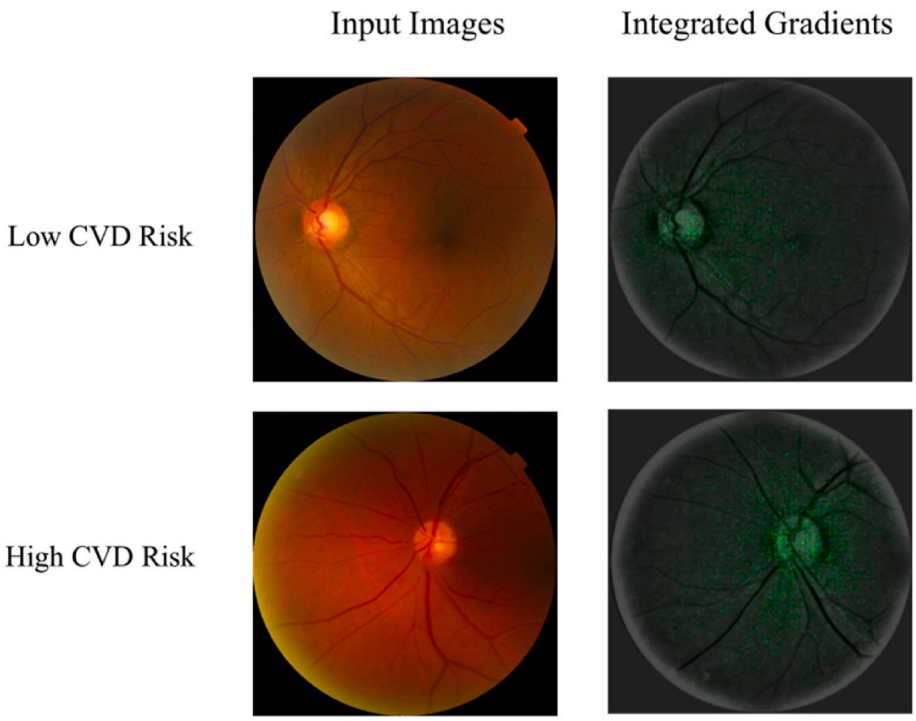

Fig. 6. The attention visualization of the deep learning model for predicting Reti-WHO risk scores based on retinal images. The highlighted green regions represent the areas of focus for the model. (For interpretation of the references to color in this figure legend, the reader is referred to the Web version of this article.)

Declaration of competing interest

The authors have no conflicts of interest to declare that are relevant to the content of this article.

Acknowledgment

During the writing of this work, the authors employed ChatGPT3.5 to receive a more professional expression. After using ChatGPT, the authors meticulously reviewed and enhanced the content as needed and took full responsibility for the content of the publication.

References

[1] Heidenreich PA, et al. Forecasting the future of cardiovascular disease in the United States: a policy statement from the American Heart Association. Circulation 2011;123(8):933–44.
[2] Roth GA, et al. Global burden of cardiovascular diseases and risk factors, 1990-2019: update from the GBD 2019 study. J Am Coll Cardiol 2020;76(25):2982–3021.
[3] Zadeh FJ, et al. Do exosomes play role in cardiovascular disease development in hematological malignancy? Mol Biol Rep 2020;47:5487–93.
[4] Zadeh FJ, et al. The role of exogenous Fibrinogen in cardiac surgery: stop bleeding or induce cardiovascular disease. Mol Biol Rep 2020;47(10):8189–98.
[5] Sheikh M, Ostadrahimi P, Shahraki E. Evaluation of in-hospital mortality of acute coronary syndrome based on blood glucose at admission. J Diabetes Nurs 2021;9(2):1408–18.
[6] Petruzzo M, et al. The Framingham cardiovascular risk score and 5-year progression of multiple sclerosis. Eur J Neurol 2021;28(3):893–900.
[7] Piepoli MF, et al. 2016 European guidelines on cardiovascular disease prevention in clinical practice: the sixth joint task force of the European society of cardiology and other societies on cardiovascular disease prevention in clinical practice (constituted by representatives of 10 societies and by invited experts)Developed with the special contribution of the European association for cardiovascular prevention & rehabilitation (EACPR). Eur Heart J 2016;37(29):2315–81.
[8] Grundy SM, et al. 2018 AHA/ACC/AACVPR/AAPA/ABC/ACPM/ADA/AGS/APhA/ASPC/NLA/PCNA guideline on the management of blood cholesterol: a report of the American college of cardiology/American heart association task force on clinical practice guidelines. Circulation 2019;139(25):e1082–143.
[9] Lloyd-Jones DM. Cardiovascular risk prediction: basic concepts, current status, and future directions. Circulation 2010;121(15):1768–77.
[10] Cooney MT, Dudina AL, Graham IM. Value and limitations of existing scores for the assessment of cardiovascular risk: a review for clinicians. J Am Coll Cardiol 2009;54(14):1209–27.
[11] Alagona Jr P, Ahmad TA. Cardiovascular disease risk assessment and prevention: current guidelines and limitations. Med Clin 2015;99(4):711–31.
[12] Group WCRCW. World Health Organization cardiovascular disease risk charts: revised models to estimate risk in 21 global regions. Lancet Global Health 2019;7(10):e1332–45.
[13] Sampietro T, et al. Acute increase in ocular microcirculation blood flow upon cholesterol removal. The eyes are the window of the heart. Am J Med 2023;136(1):108–14.
[14] Huang L, et al. Exploring associations between cardiac structure and retinal vascular geometry. J Am Heart Assoc 2020;9(7):e014654.
[15] Zekavat SM, et al. Deep learning of the retina enables phenome-and genome-wide analyses of the microvasculature. Circulation 2022;145(2):134–50.
[16] Pampana LK, Rayudu MS. A review: prediction of multiple adverse health conditions from retinal images. In: 2020 IEEE Bangalore humanitarian technology conference (B-HTC). IEEE; 2020.
[17] Tan W, et al. The new era of retinal imaging in hypertensive patients. Asia Pac J Ophthalmol (Phila) 2022;11(2):149–59.
[18] Shi D, et al. A deep learning system for fully automated retinal vessel measurement in high throughput image analysis. Front Cardiovasc Med 2022;9:823436.
[19] Al-Absi HRH, et al. Cardiovascular disease diagnosis from DXA scan and retinal images using deep learning. Sensors (Basel) 2022;22(12).
[20] Liu Z, et al. Swin transformer: hierarchical vision transformer using shifted windows. In: Proceedings of the IEEE/CVF international conference on computer vision; 2021.
[21] Gopinath B, et al. Retinal vascular geometry and the prevalence of atrial fibrillation and heart failure in a clinic-based sample. Heart Lung Circ 2019;28(11):1631–7.
[22] Betzler BK, et al. Retinal vascular profile in predicting incident cardiometabolic diseases among individuals with diabetes. Microcirculation 2022;29(4–5):e12772.
[23] Sundararajan M, Taly A, Yan Q. Axiomatic attribution for deep networks. In: International conference on machine learning. PMLR; 2017.
[24] Lee YC, et al. Multimodal deep learning of fundus abnormalities and traditional risk factors for cardiovascular risk prediction. NPJ Digit Med 2023;6(1):14.
[25] Chang J, et al. Association of cardiovascular mortality and deep learning-funduscopic atherosclerosis score derived from retinal fundus images. Am J Ophthalmol 2020;217:121–30.
[26] Ankad RB, et al. Effect of short-term pranayama and meditation on cardiovascular functions in healthy individuals. Heart Views 2011;12(2):58.

[27] Adar SD, et al. Air pollution and the microvasculature: a cross-sectional assessment of in vivo retinal images in the population-based Multi-Ethnic Study of Atherosclerosis (MESA). PLoS Med 2010;7(11):e1000372.
[28] Wong TY, et al. Retinal microvascular abnormalities and their relationship with hypertension, cardiovascular disease, and mortality. Surv Ophthalmol 2001;46(1):59–80.
[29] Roy MS, Klein R, Janal MN. Relationship of retinal vessel caliber to cardiovascular disease and mortality in African Americans with type 1 diabetes mellitus. Arch Ophthalmol 2012;130(5):561–7.